

Supporting Information

Design and chemical synthesis of a novel coumarin-based framework as a potential chemosensor of a neurotoxic insecticide, azamethiphos

Aman K.K. Bhasin^{a*}, Pushap Raj^b, Pooja Chauhan^c, Sanjay K. Mandal^d, Savita Chaudhary^c
Narinder Singh^b, Navneet kaur^c

^aDAV College, Sector 10, Chandigarh (India)-160010

^bDepartment of Chemistry, Indian Institute Technology Ropar, Punjab, 140001, India.

^cDepartment of Chemistry, Panjab University Chandigarh 160014, India

^dDepartment of Chemical Sciences, Indian Institute of Science Education and Research, Sector 81, Manauli PO, S.A.S. Nagar, Mohali, Punjab, 140306, India

**Corresponding author* (Aman KK Bhasin); *E-mail:* akkb8785@gmail.com; *Tel:* +91-8557895390.

Contents

Figure S1. ^1H NMR spectrum of ligand L in dms-*d*6.

Figure S2. ^{13}C NMR spectrum of ligand L in dms-*d*6.

Figure S3. Mass spectrum of ligand L determined by electrospray ionization technique (ESI-MS).

Figure S4. Competitive binding experiment between Cu^{2+} and organic nanoparticles **A1** in the presence of competing metal ion pool.

Figure S5. Stern-volmer plot for determination of association constant (K_a) between Cu^{2+} and organic nanoparticles, **A1**.

Figure S6. Job plot to determine the stoichiometry of the chemical coordination between the host ligand A1 and guest metal ion Cu^{2+} .

Figure S7.1 ^1H NMR titration of **A1** in presence and absence of Cu^{2+} in dms-*d*6 (H^a and H^b denote hydroxyl proton and iminic hydrogen of **A1**, respectively)

Figure S7.2 ^1H NMR titration of **A1** in presence of Cu^{2+} and azamethiphos in dms-*d*6 (H^a and H^b denote hydroxyl proton and iminic hydrogen of **A1**, respectively)

Figure S8. Benesi-Hildebrand plot to determine the binding constant between Cu^{2+} ·**A1** with azamethiphos where F_0 and F denote the fluorescence emission intensity of the copper-bound receptor complex Cu^{2+} ·**A1** in the absence and presence of azamethiphos (analyte), respectively. $[G]$ represents the molar concentration of azamethiphos.

Figure S9. Job plot to determine the stoichiometry of the binding interaction between the host complex Cu^{2+} ·**A1** and azamethiphos (analyte). $[H]$ and $[G]$ represent the molar concentration of the host complex Cu^{2+} ·**A1** and azamethiphos, respectively

Figure S10. Competitive binding experiment of copper-ligand ensemble (Cu^{2+} ·**A1**) towards azamethiphos in the presence of select organophosphate pesticides

Figure S11. ^{31}P NMR spectrum of azamethiphos in the presence and absence of copper-ligand ensemble, Cu^{2+} ·**A1**

Figure S12. Fluorescence profile of Cu^{2+} ·**A1** ($50\ \mu\text{M}$; $\lambda_{\text{em}} = 430\text{nm}$) in presence of a library of select anions ($50\ \mu\text{M}$) in aqueous medium

Figure S13. Fluorescence titration studies of azamethiphos ($\lambda_{\text{em}} = 330\text{ nm}$) with Cu^{2+} ($0- 50\ \mu\text{M}$)

Figure S14. Fluorescence profile of azamethiphos ($\lambda_{\text{em}} = 330\text{ nm}$) in the presence of (i) Cu^{2+} (ii) ligand (**A1**) and (iii) ligand-copper ensemble (**A1**· Cu^{2+})

Figure S15. Cyclical fluctuations in fluorescence intensity ($\lambda_{em} = 430$ nm) of title ligand **A1** upon sequential dosage of azamethiphos (100 - 40 μ M) and Cu^{2+} (50-10 μ M) in an alternate pattern

Figure S16. Fluorescence studies in deionized water and select real water samples (tap water, rain water and well water) of (a) **A1** ($\lambda_{em} = 430$ nm) upon spiking with Cu^{2+} (10, 20, 30, 40 and 50 μ M) and (b) **A1**· Cu^{2+} ($\lambda_{em} = 440$ nm) upon spiking with azamethiphos (10, 20, 30, 40 and 50 μ M)

Figure S17. Fully labeled molecular structure of ligand L

Table S1. Crystal data and structure refinement for ligand L

Table S2. Selected bond lengths (\AA) of L

Table S3. Selected bond angles (A°) of L

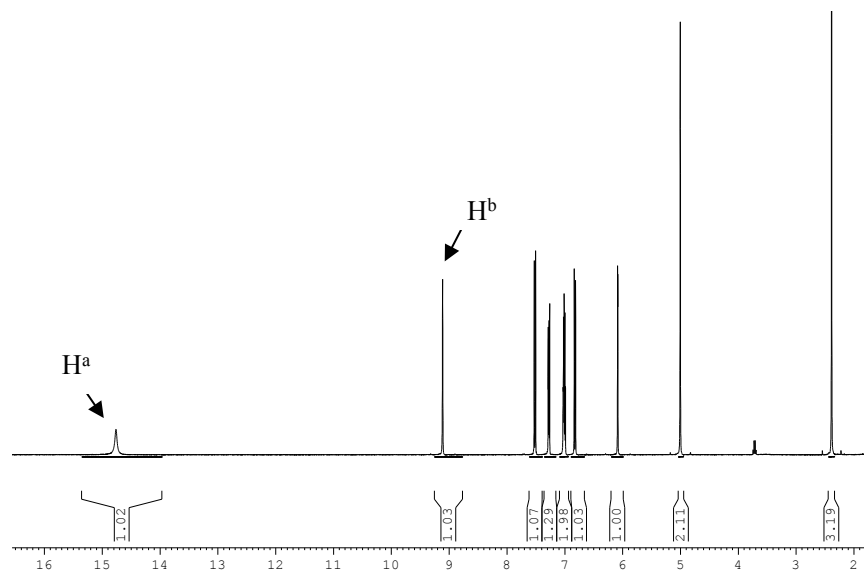


Figure S1. ^1H NMR spectrum of ligand L in $\text{dms-}d_6$ (H^a and H^b denote hydroxyl and iminic protons, respectively).³¹

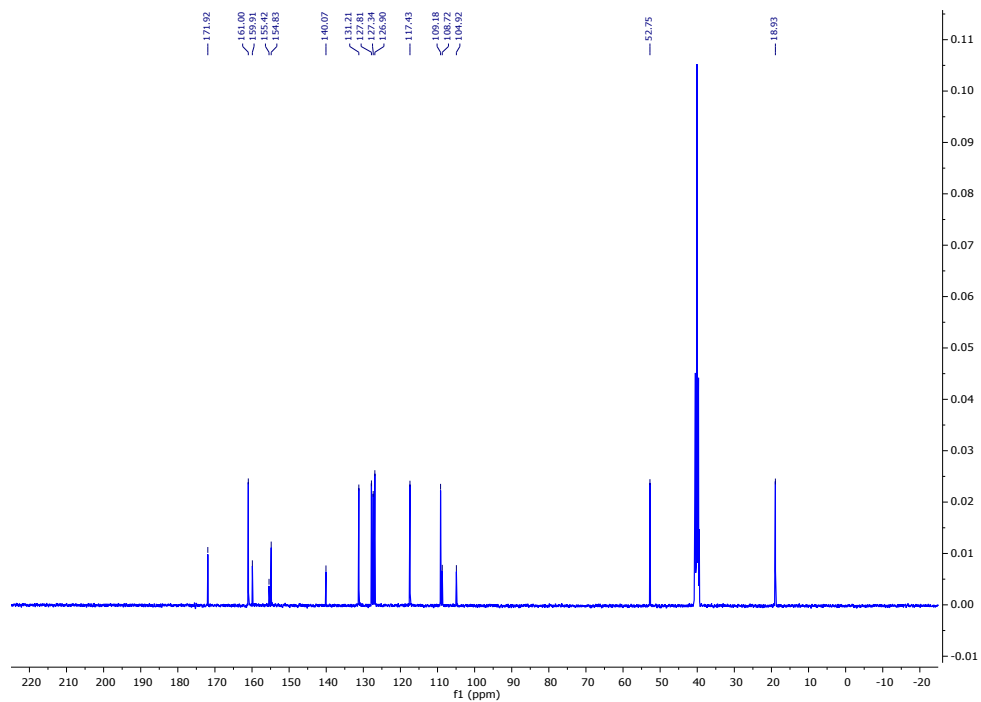


Figure S2. ^{13}C NMR spectrum of ligand L in $\text{dms-}d_6$.

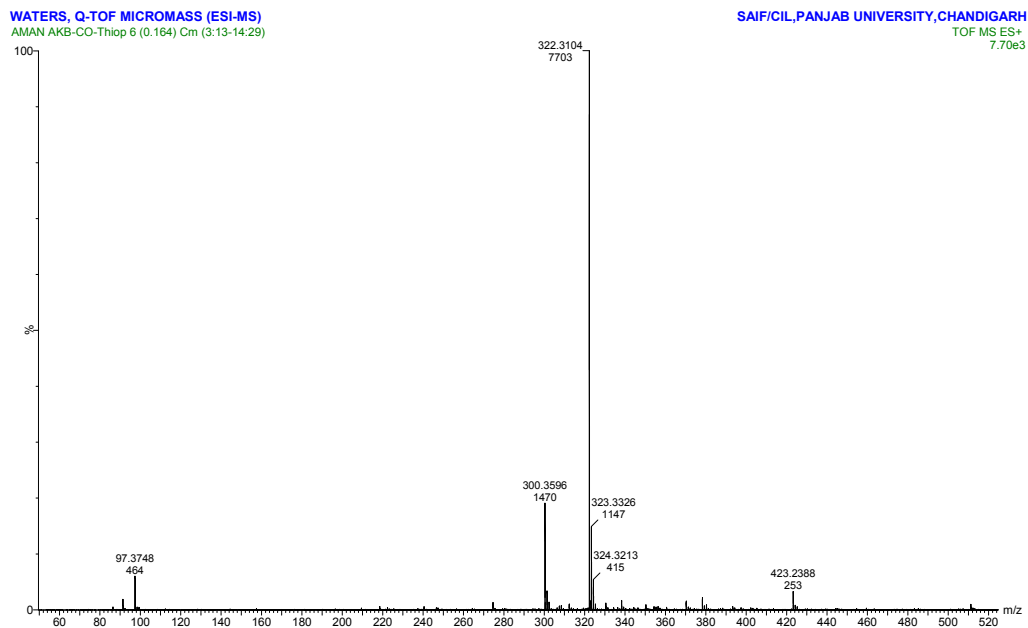


Figure S3. Mass spectrum of ligand L via electrospray ionization technique (positive mode)

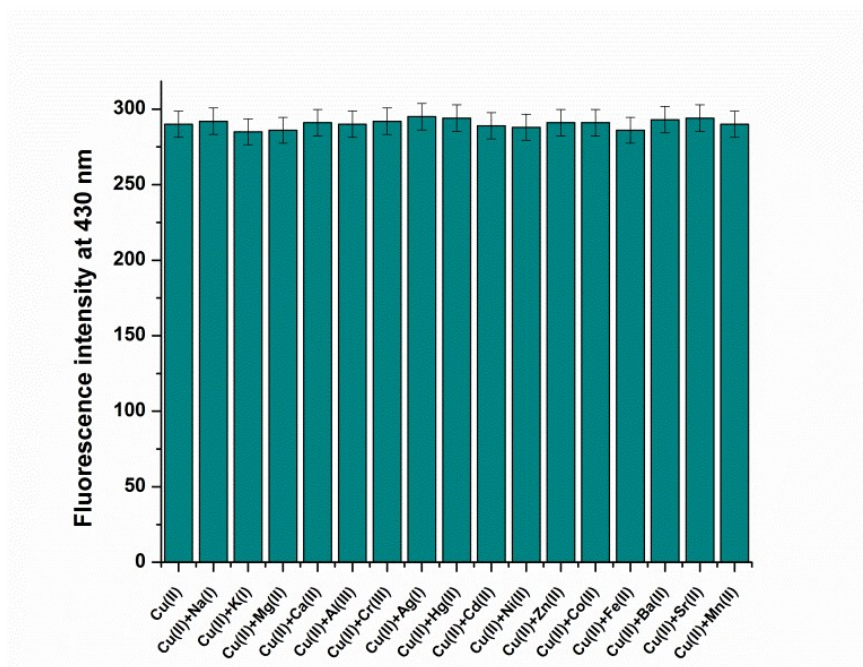


Figure S4. Competitive binding experiment of title ligand **A1** with Cu^{2+} in the presence of competing select metal ions.

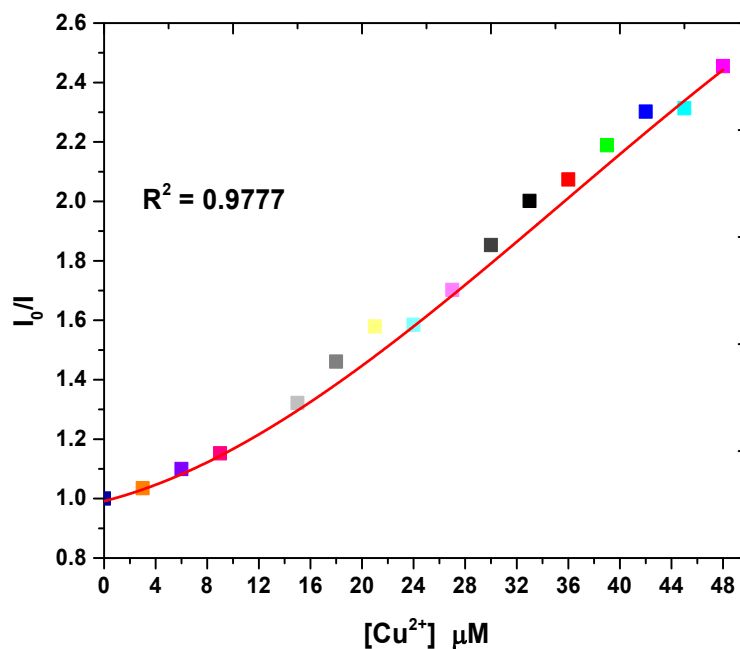


Figure S5. Stern-Volmer plot for determination of association constant (K_a) between Cu^{2+} and organic nanoparticles **A1**

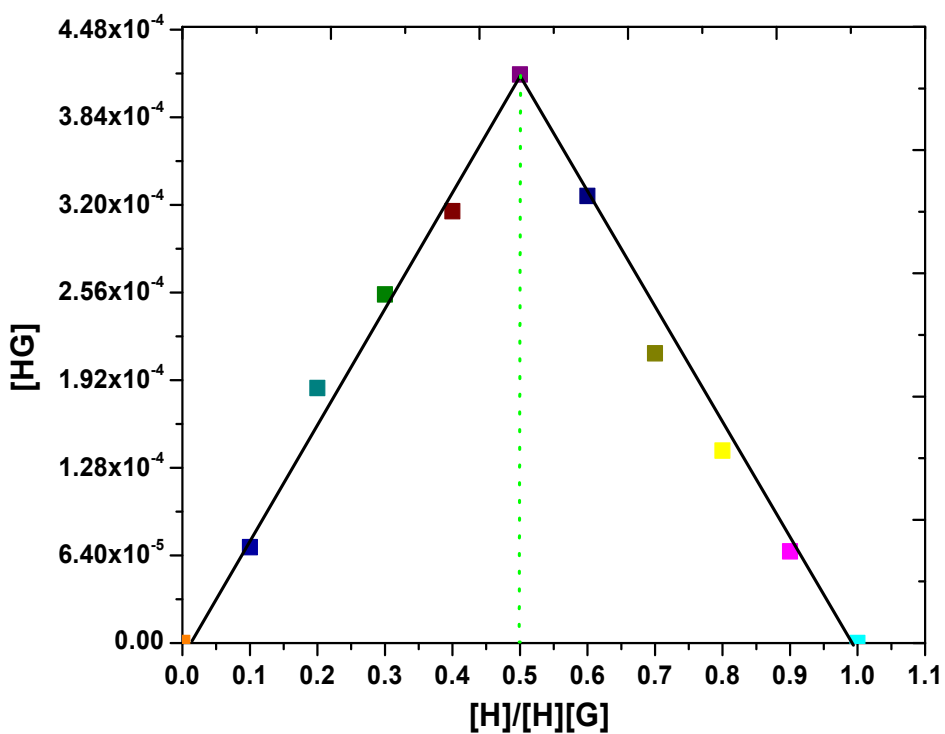
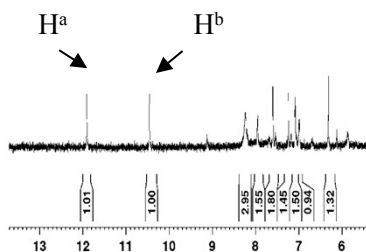


Figure S6. Job plot to determine the stoichiometry of the chemical coordination between the host ligand **A1** and guest metal ion Cu^{2+} .

Copper-bound receptor ligand A1



Copper-free receptor ligand A1

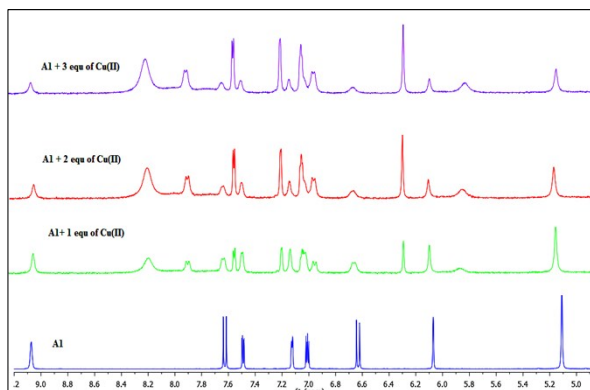
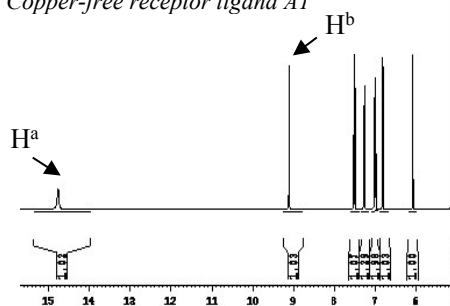


Figure S7.1 ^1H NMR titration of **A1** in presence and absence of Cu^{2+} in $\text{dms}\text{-}d_6$ (H^a and H^b denote hydroxyl proton and iminic hydrogen of **A1**, respectively)

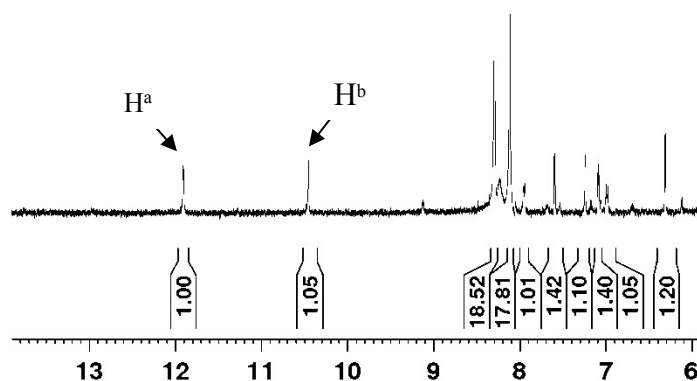


Figure S7.2 ^1H NMR titration of **A1** in presence of Cu^{2+} and azamethiphos in $\text{dms}\text{-}d_6$ (H^a and H^b denote hydroxyl proton and iminic hydrogen of **A1**, respectively)

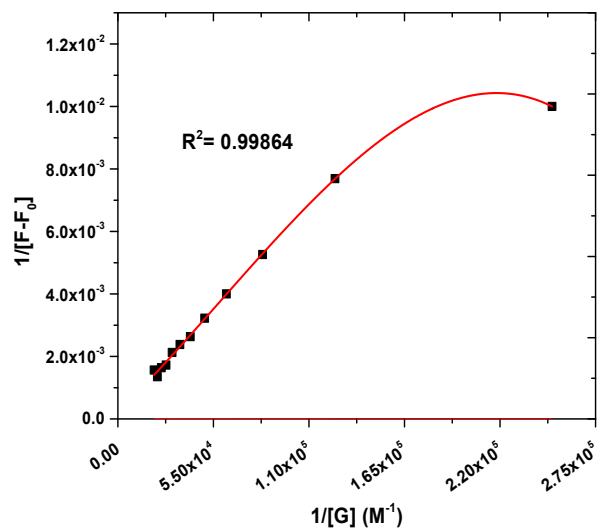


Figure S8. Benesi-Hildebrand plot to determine the binding constant between $\text{Cu}^{2+}\text{-A1}$ with azamethiphos where F_0 and F denote the fluorescence emission intensity of the copper-bound receptor complex $\text{Cu}^{2+}\text{-A1}$ in the absence and presence of azamethiphos (analyte), respectively. $[G]$ represents the molar concentration of azamethiphos.

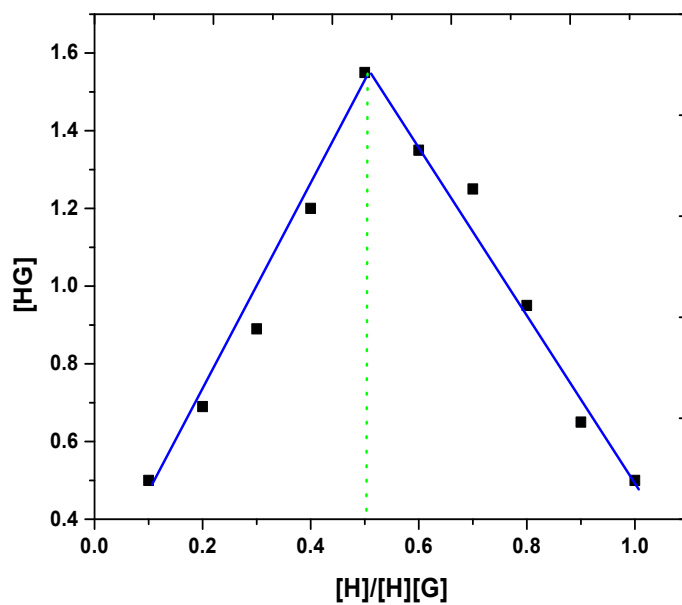


Figure S9. Job plot to determine the stoichiometry of the binding interaction between the host complex $\text{Cu}^{2+}\text{-A1}$ and azamethiphos (analyte). $[H]$ and $[G]$ represent the molar concentration of the host complex $\text{Cu}^{2+}\text{-A1}$ and azamethiphos, respectively

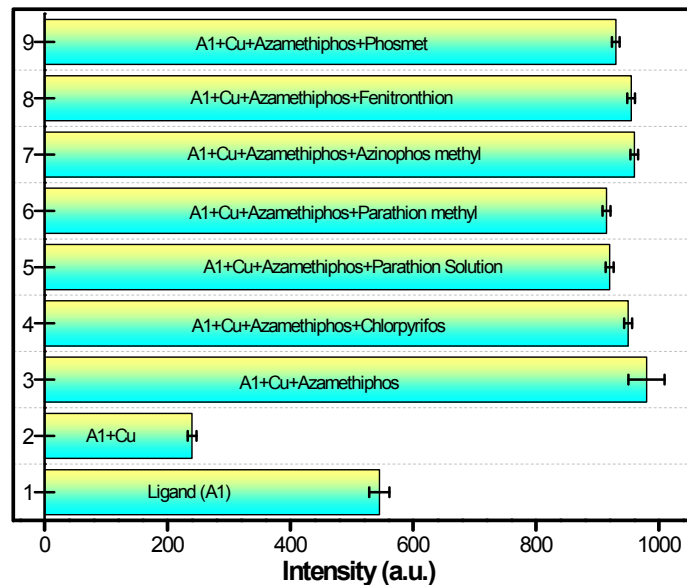


Figure S10. Competitive binding experiment of copper:ligand ensemble ($\text{Cu}^{2+} \cdot \mathbf{A1}$; $\lambda_{\text{em}} = 440 \text{ nm}$) towards azamethiphos in the presence of select organophosphate pesticides

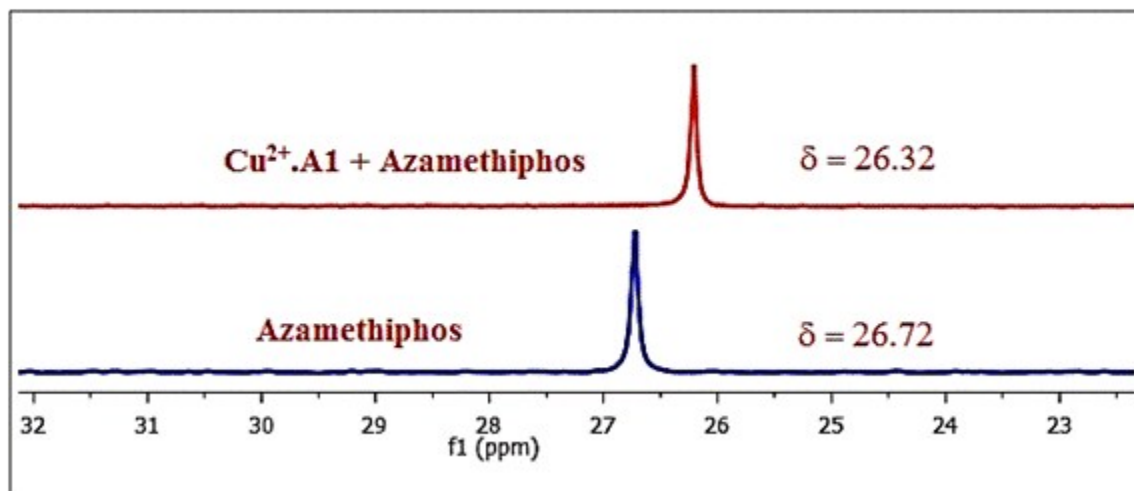


Figure S11. ^{31}P NMR spectrum of azamethiphos in the presence and absence of copper-ligand ensemble, $\text{Cu}^{2+} \cdot \mathbf{A1}$

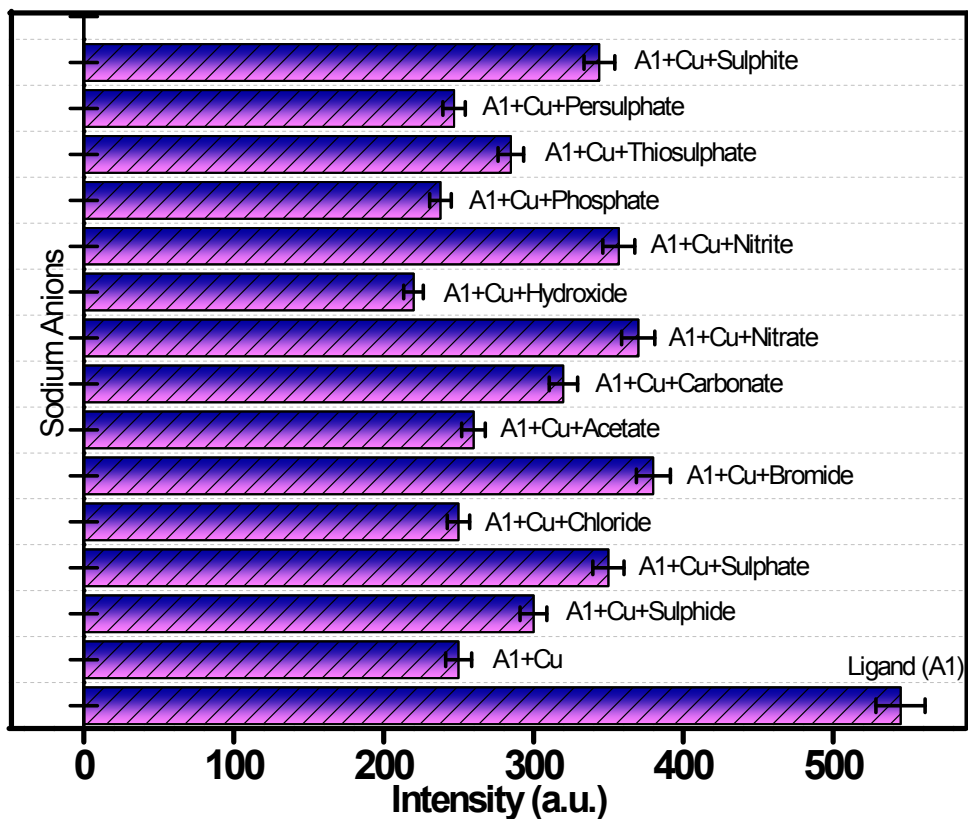


Figure S12. Fluorescence profile of Cu^{2+} -A1 ($50\mu\text{M}$; $\lambda_{\text{em}} = 430\text{nm}$) in presence of a library of select anions ($50\mu\text{M}$) in aqueous medium.

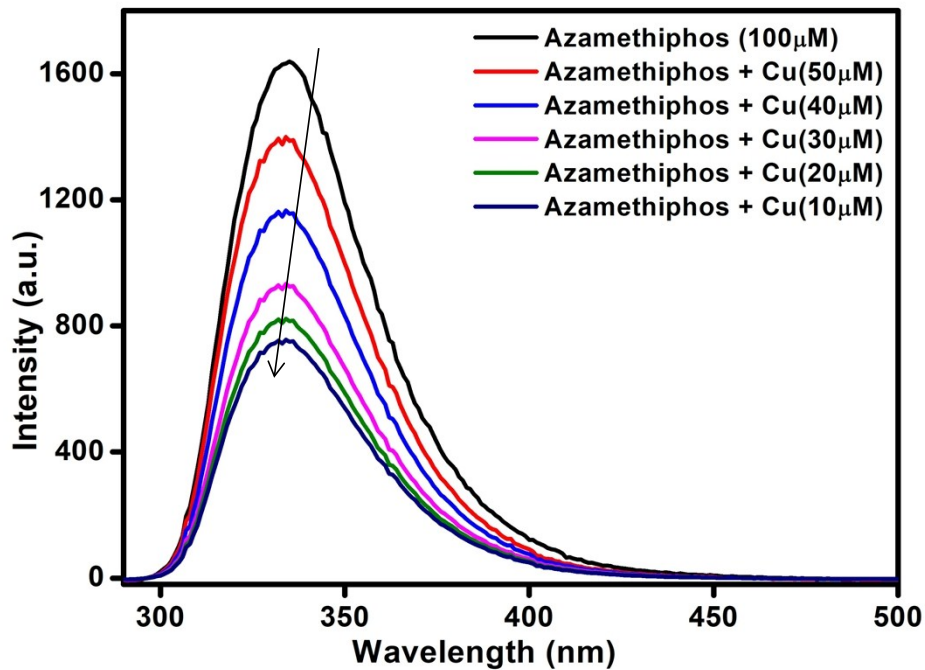


Figure S13. Fluorescence titration studies of azamethiphos (100 μM; $\lambda_{em} = 330$ nm) with Cu²⁺ (0-50 μM)

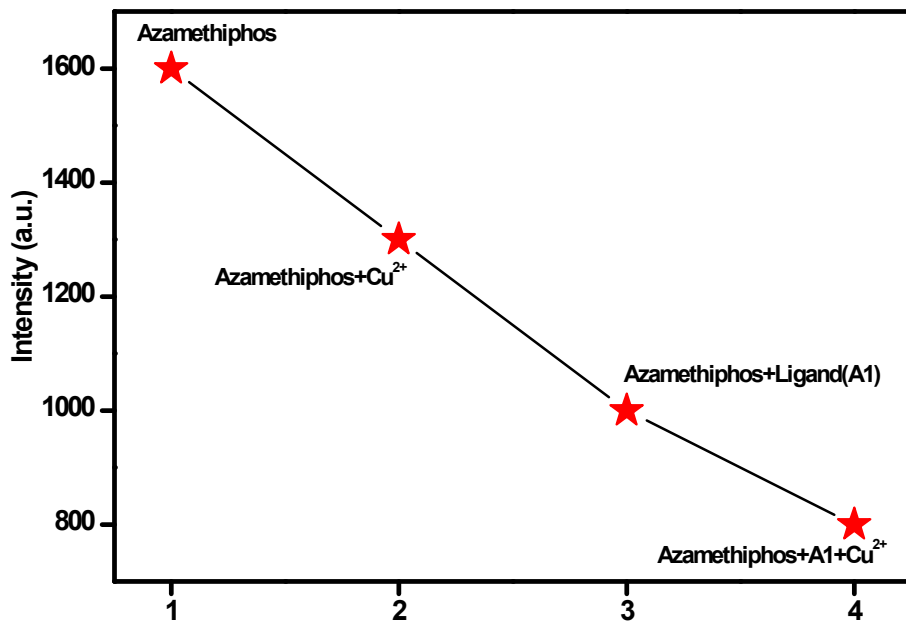


Figure S14. Fluorescence profile of azamethiphos ($\lambda_{em} = 330$ nm) in the presence of (i) Cu²⁺ (ii) ligand (A1) and (iii) ligand-copper ensemble (A1·Cu²⁺)

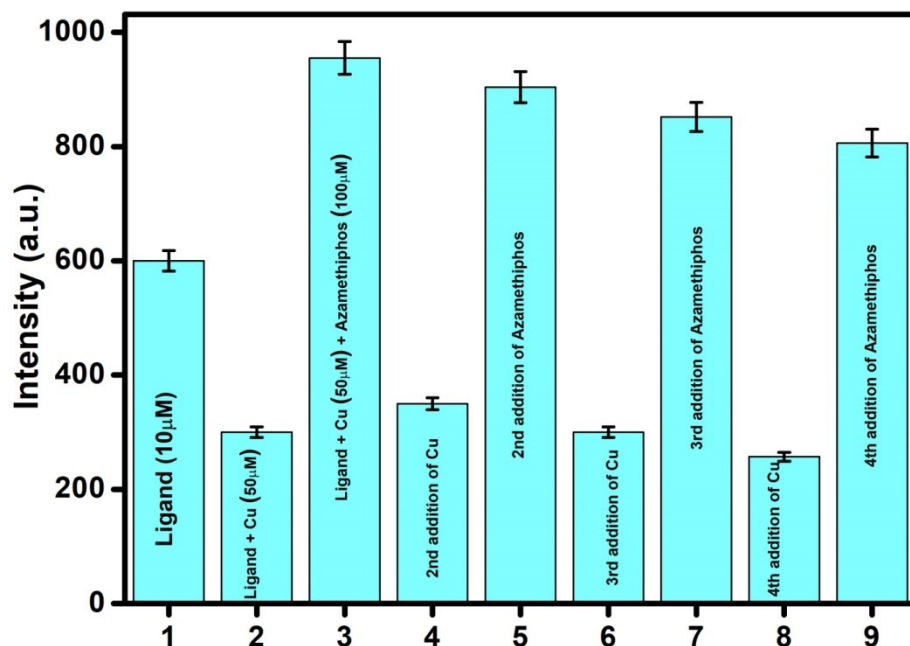


Figure S15. Cyclical fluctuations in fluorescence intensity of ligand A1 ($\lambda_{em} = 430$ nm; 10 μ M) upon sequential dosage of azamethiphos (100 - 40 μ M) and Cu²⁺ (50-20 μ M) in an alternate pattern.

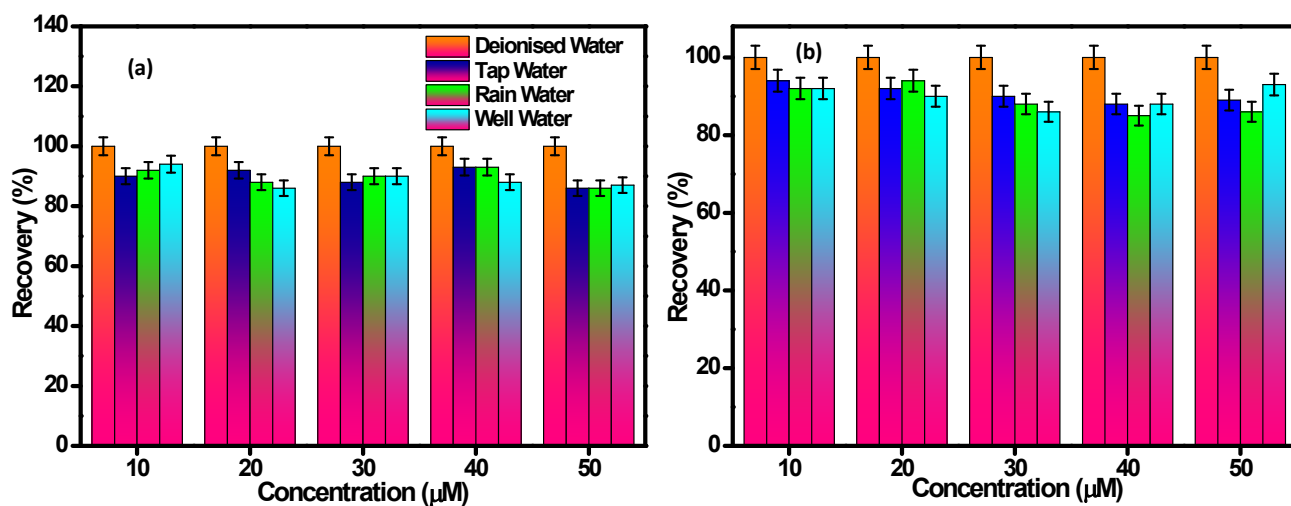


Figure S16. Fluorescence studies in deionized water and select real water samples (tap water, rain water and well water) of (a) A1 ($\lambda_{em} = 430$ nm) upon spiking with Cu²⁺ (10, 20, 30, 40 and 50 μ M) and (b) A1Cu²⁺ ($\lambda_{em} = 440$ nm) upon spiking with azamethiphos (10, 20, 30, 40 and 50 μ M)

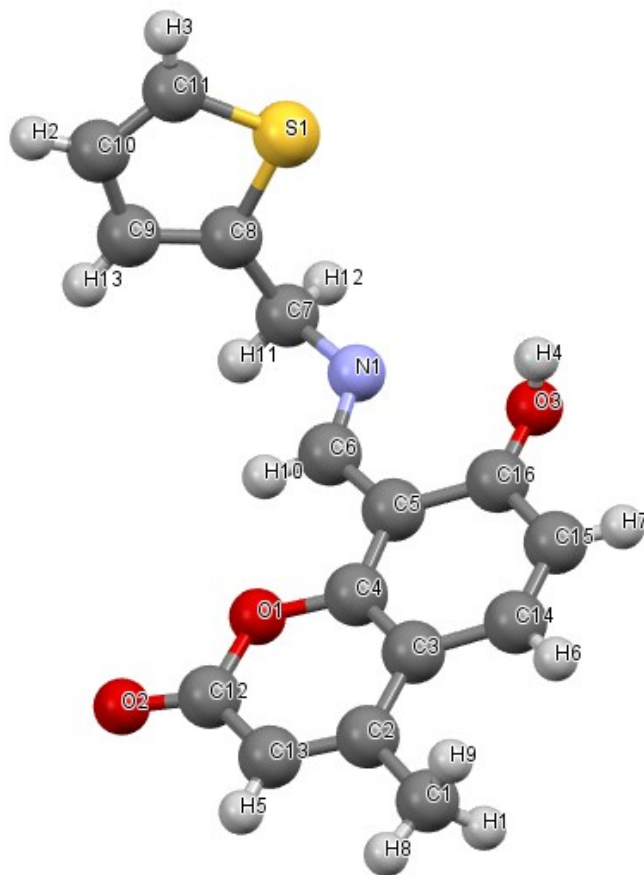


Figure S17. Fully labeled molecular structure of ligand L

Table S1. Crystal data and structure refinement for ligand L

Chemical formula	C₁₆H₁₃NO₃S	
Formula weight	299.33	
Temperature	296(2) K	
Wavelength	0.71073 Å	
Crystal system	Triclinic	
Space group	P -1	
Unit cell dimensions	a = 7.518(7) Å	α = 70.671(10)°
	b = 9.118(9) Å	β = 71.668(11)°
	c = 11.293(11) Å	γ = 78.323(11)°
Volume	689.2(11) Å³	
Z	2	
Density (calculated)	1.442 g/cm³	
Absorption coefficient	0.244 mm⁻¹	
F(000)	312	

Theta range for data collection	1.98 to 25.16°	
Index ranges	-8<=h<=8, -10<=k<=10, -13<=l<=13	
Reflections collected	8677	
Independent reflections	2461 [R(int) = 0.0180]	
Coverage of independent reflections	99.9%	
Absorption correction	multi-scan	
Structure solution technique	direct methods	
Structure solution program	SHELXS-97 (Sheldrick, 2008)	
Refinement method	Full-matrix least-squares on F²	
Refinement program	SHELXL-97 (Sheldrick, 2008)	
Function minimized	Σ w(F_o² - F_c²)²	
Data / restraints / parameters	2461 / 0 / 192	
Goodness-of-fit on F ²	1.051	
Final R indices	2186 data; I > 2σ (I) all data	R1 = 0.0460, wR2 = 0.1408 R1 = 0.0503, wR2 = 0.1461
Weighting scheme	w=1/[σ²(F_o²)+(0.0917P)²+0.2923P] where P=(F_o²+2F_c²)/3	
Largest diff. peak and hole	0.652 and -0.494 eÅ⁻³	

Table S2. Bond lengths (Å) of L

S1-C8	1.718(3)	S1-C11	1.716(3)
O1-C4	1.370(2)	O1-C12	1.394(2)
O2-C12	1.210(3)	O3-C16	1.256(3)
O3-H4	0.82	N1-C6	1.301(3)
N1-C7	1.476(2)	C1-C2	1.498(3)
C1-H8	0.96	C1-H9	0.96
C1-H1	0.96	C2-C13	1.356(3)
C2-C3	1.437(3)	C3-C4	1.385(3)
C3-C14	1.431(3)	C4-C5	1.418(3)
C5-C6	1.413(3)	C5-C16	1.457(3)
C6-H10	0.93	C7-C8	1.498(3)
C7-H11	0.97	C7-H12	0.97
C8-C9	1.381(3)	C9-C10	1.406(4)
C9-H13	0.93	C10-C11	1.332(4)
C10-H2	0.93	C11-H3	0.93
C12-C13	1.428(3)	C13-H5	0.93
C14-C15	1.353(3)	C14-H6	0.93

C15-C16	1.441(3)	C15-H7	0.93
---------	-----------------	--------	-------------

Table S3. Bond angles (°) of L

C8-S1-C11	92.10(13)	C4-O1-C12	121.98(14)
C16-O3-H4	109.5	C6-N1-C7	122.80(16)
C2-C1-H8	109.5	C2-C1-H9	109.5
H8-C1-H9	109.5	C2-C1-H1	109.5
H8-C1-H1	109.5	H9-C1-H1	109.5
C13-C2-C3	119.12(17)	C13-C2-C1	120.65(18)
C3-C2-C1	120.23(18)	C4-C3-C14	116.83(18)
C4-C3-C2	118.65(18)	C14-C3-C2	124.51(17)
O1-C4-C3	121.11(17)	O1-C4-C5	115.37(15)
C3-C4-C5	123.53(17)	C6-C5-C4	120.25(17)
C6-C5-C16	121.06(17)	C4-C5-C16	118.68(16)
N1-C6-C5	124.29(17)	N1-C6-H10	117.9
C5-C6-H10	117.9	N1-C7-C8	112.65(16)
N1-C7-H11	109.1	C8-C7-H11	109.1
N1-C7-H12	109.1	C8-C7-H12	109.1
H11-C7-H12	107.8	C9-C8-C7	126.54(19)
C9-C8-S1	110.08(16)	C7-C8-S1	123.37(16)
C8-C9-C10	112.5(2)	C8-C9-H13	123.7
C10-C9-H13	123.7	C11-C10-C9	113.8(2)
C11-C10-H2	123.1	C9-C10-H2	123.1
C10-C11-S1	111.5(2)	C10-C11-H3	124.2
S1-C11-H3	124.3	O2-C12-O1	115.57(17)
O2-C12-C13	127.85(18)	O1-C12-C13	116.58(17)
C2-C13-C12	122.53(18)	C2-C13-H5	118.7
C12-C13-H5	118.7	C15-C14-C3	122.29(17)
C15-C14-H6	118.9	C3-C14-H6	118.9
C14-C15-C16	122.17(18)	C14-C15-H7	118.9
C16-C15-H7	118.9	O3-C16-C15	122.47(18)
O3-C16-C5	121.03(17)	C15-C16-C5	116.49(18)